Contribution from the Department of Chemistry, Harvard University, Cambridge, Massachusetts 02138, and the Francis Bitter National Magnet Laboratory, Massachusetts Institute of Technology, Cambridge, Massachusetts 02139

Alternative Spin States in Synthetic Analogues of Biological [4Fe-4S]$^+$ Clusters: Further Cases of Variable Ground States and the Structure of $(Et_4N)_3[Fe_4S_4(S\text{-}o\text{-}C_6H_4StBu)_4]$, Containing a Reduced Cluster with a Compressed Tetragonal Distortion

M. J. Carney,[†] G. C. Papaefthymiou,[‡] R. B. Frankel,[‡,§] and R. H. Holm*[,†]

Received September 7, 1988

Previous work has shown that the cubane-type reduced clusters $[Fe_4S_4(SR)_4]^{3-}$, synthetic analogues of sites in reduced ferredoxins and other proteins, as polycrystalline samples can exist in three ground-state situations: (i) pure $S = {}^1/_2$ or $S = {}^3/_2$; (ii) physical mixtures of $S = {}^1/_2$ and ${}^3/_2$, where spectroscopic and magnetic properties are summations of the properties of the two states; (iii) "spin-admixed", where the properties are not summations but arise from a different electronic state. One example of a category iii cluster, $(Et_4N)_3[Fe_4S_4(SCH_2Ph)_4]$ (**5**), has been documented previously. Evidence for the placement of the following cluster compounds in the spin-admixed category is presented here: $(Et_4N)_3[Fe_4S_4(S\text{-}o\text{-}C_6H_4StBu)_4]$ (**1**), $(Et_4N)_3[Fe_4S_4(StBu)_4]\cdot MeCN$ (**2**), $(Et_3NMe)_3[Fe_4S_4(SPh)_4]$ (**3**), $(Me_4N)_3[Fe_4S_4(SEt)_4]$ (**4**). Crystal structures of all but **1** have been previously reported. Compound **1** crystallizes in monoclinic space group $P2_1/n$ with $a = 17.467$ (7) Å, $b = 15.011$ (7) Å, $c = 30.413$ (9) Å, $\beta = 94.31$ (3)°, and $Z = 4$. With use of 4319 unique data ($F_o^2 > 3\sigma(F_o^2)$), the structure was refined to R (R_w) = 7.93% (8.07%). The [4Fe-4S]$^+$ core of the cluster exhibits a compressed tetragonal distortion from idealized T_d symmetry with four short (mean 2.265 (19) Å) and eight long (mean 2.319 (23) Å) Fe–S bonds parallel and perpendicular, respectively, to an idealized $\bar{4}$ axis bisecting opposite faces of the core. The very bulky thiolate ligands are oriented so as to place the *o*-S*t*Bu group as far from the core as possible in an overall arrangement indicative of conformations arising mainly from intracluster interactions. The compressed distortion of this cluster is considered intrinsic. Low-temperature magnetic susceptibility, magnetization, and Mössbauer spectroscopic results are reported. The magnetic data for **1**–**3** are not inconsistent with a physical mixture of spin states; the magnetism of **4** is somewhat anomalous. However, the Mössbauer spectra of **1**–**4**, as that of **5**, in an applied field of 60 kOe at 4.2 K, lack the features at ca. +3 and −2 mm/s characteristic of the $S = {}^1/_2$ state, whose magnetically perturbed Mössbauer spectra in synthetic and biological clusters are essentially invariant. Structural data for nine reduced clusters, determined at ambient temperature, are schematically depicted. The existence of *five* modes of core distortion indicates a pronounced sensitivity of structure to crystal environment. The most frequent distortions are compressed tetragonal (**1**, **2**, **4**) and elongated tetragonal (**3** plus two others). The present results, when taken with those reported recently from these laboratories, provide further evidence for the existence of three types of ground-state behavior of reduced clusters and show that there does not exist a unique core distortion or a unique set of thiolate ligand conformations (or a combination of the two) that is indicative of spin-admixed behavior in **1**–**5**. Any correlation between fine details of structure and spin ground states may require determination of crystal structures in the same cryogenic temperature range where magnetic and spectroscopic properties have been measured.

Introduction

A substantial portion of our prior research on cubane-type iron–sulfur clusters containing the [4Fe-4S]$^+$ core oxidation level[1-12] has demonstrated that the synthetic analogues $[Fe_4S_4(SR)_4]^{3-}$ of native reduced clusters possess a structural and spin state variability that is far more extensive and complex than for biological and synthetic clusters containing the [4Fe-4S]$^{2+,3+}$ cores.[13-15] Some five distortions from idealized cubic core symmetry have been identified by X-ray crystallography, with an associated variety of ground-state electronic properties. We have shown that polycrystalline synthetic clusters can exist in the following situations: (i) as clusters with pure $S = {}^1/_2$ or ${}^3/_2$ ground states; (ii) as physical mixtures of clusters with pure $S = {}^1/_2$ and $S = {}^3/_2$ ground states; (iii) as "spin-admixed" clusters, which have spectroscopic properties that are not simple summations of pure $S = {}^1/_2$ and $S = {}^3/_2$ ground states. This categorization has been arrived at by the study of some 16 compounds containing 13 different reduced clusters $[Fe_4S_4(SR)_4]^{3-}$. One matter that has clearly emerged is the extraordinary and unpredictable sensitivity of the spin ground state to those extrinsic factors that regulate the detailed cluster structure in the solid state. In frozen solutions, where such perturbations are largely removed, all synthetic clusters that we have examined exist as physical mixtures of spin states, albeit in different proportions.

Over the last several years, it has also become clear that biological [4Fe-4S]$^+$ clusters can deviate from what had been long believed to be the usual (or only) ground state, a spin doublet. The best characterized examples include the [4Fe-4Se]$^+$ clusters of the selenium-reconstituted ferredoxin from *Clostridium pasteurianum* ($Se\text{-}Fd_{red}$)[16-23] and the [4Fe-4S]$^+$ centers of the Fe proteins of the Mo- and V-containing *Azotobacter* nitrogenase systems ($Av2$[24,25] and $Av2'$[26]). Each of these proteins exists as

[†] Harvard University.
[‡] Massachusetts Institute of Technology.
[§] Present address: Department of Physics, California Polytechnic State University, San Luis Obispo, CA 93407.

(1) Laskowski, E. J.; Frankel, R. B.; Gillum, W. O.; Papaefthymiou, G. C.; Renaud, J.; Ibers, J. A.; Holm, R. H. *J. Am. Chem. Soc.* **1978**, *100*, 5322.
(2) Hagen, K. S.; Watson, A. D.; Holm, R. H. *Inorg. Chem.* **1984**, *23*, 2984.
(3) Berg, J. M.; Hodgson, K. O.; Holm, R. H. *J. Am. Chem. Soc.* **1979**, *101*, 4568.
(4) Stephan, D. W.; Papaefthymiou, G. C.; Frankel, R. B.; Holm, R. H. *Inorg. Chem.* **1983**, *22*, 1550.
(5) Laskowski, E. J.; Reynolds, J. G.; Frankel, R. B.; Foner, S.; Papaefthymiou, G. C.; Holm, R. H. *J. Am. Chem. Soc.* **1979**, *101*, 6562.
(6) Papaefthymiou, G. C.; Laskowski, E. J.; Frota-Pessôa, S.; Frankel, R. B.; Holm, R. H. *Inorg. Chem.* **1982**, *21*, 1723.
(7) Cambray, J.; Lane, R. W.; Wedd, A. G.; Johnson, R. W.; Holm, R. H. *Inorg. Chem.* **1977**, *16*, 2565.
(8) Reynolds, J. G.; Laskowski, E. J.; Holm, R. H. *J. Am. Chem. Soc.* **1978**, *100*, 5315.
(9) Reynolds, J. G.; Coyle, C. L.; Holm, R. H. *J. Am. Chem. Soc.* **1980**, *102*, 4350.
(10) Carney, M. J.; Holm, R. H.; Papaefthymiou, G. C.; Frankel, R. B. *J. Am. Chem. Soc.* **1986**, *108*, 3519.
(11) Carney, M. J.; Papaefthymiou, G. C.; Whitener, M. A.; Spartalian, K.; Frankel, R. B.; Holm, R. H. *Inorg. Chem.* **1988**, *27*, 346.
(12) Carney, M. J.; Papaefthymiou, G. C.; Spartalian, K.; Frankel, R. B.; Holm, R. H. *J. Am. Chem. Soc.* **1988**, *110*, 6084.
(13) Berg, J. M.; Holm, R. H. In *Iron-Sulfur Proteins*; Spiro, T. G., Ed.; Wiley-Interscience: New York, 1982; Chapter 1.
(14) (a) Cammack, R.; Dickson, D. P. E.; Johnson, C. E. In *Iron-Sulfur Proteins*; Lovenberg, W., Ed.; Academic Press: New York, 1977; Vol. III, Chapter 8. (b) Sweeney, W. V.; Rabinowitz, J. C. *Annu. Rev. Biochem.* **1980**, *49*, 39. (c) Thomson, A. J. *Top. Mol. Struct. Biol.* **1985**, *6* (Metalloproteins, part 1), 79.
(15) (a) O'Sullivan, T.; Millar, M. M. *J. Am. Chem. Soc.* **1985**, *107*, 4096. (b) Papaefthymiou, V.; Millar, M. M.; Münck, E. *Inorg. Chem.* **1986**, *25*, 3010.
(16) Moulis, J.-M.; Auric, P.; Gaillard, J.; Meyer, J. *J. Biol. Chem.* **1984**, *259*, 11396.
(17) Gaillard, J.; Moulis, J.-M.; Auric, P.; Meyer, J. *Biochemistry* **1986**, *25*, 464.
(18) Meyer, J.; Moulis, M.-M. *Biochem. Biophys. Res. Commun.* **1981**, *103*, 667.
(19) Moulis, J.-M.; Meyer, J. *Biochemistry* **1982**, *21*, 4762.

0020-1669/89/1328-1497$01.50/0

a mixture of (at least) $S = {}^1/_2$ and $S = {}^3/_2$ ground-state clusters. For $[4Fe\text{-}4S]^+$ clusters, the proportion of the two is dependent on the medium and the chemical state of the protein. Furthermore, EPR and Mössbauer spectroscopic evidence suggests that certain $[4Fe\text{-}4Se]^+$ clusters in Se-Fd_{red}[16,17,22,23] and $[4Fe\text{-}4S]^+$ clusters in ATP-bound Av2 populate states with $S > {}^3/_2$.[25]

The foregoing brief summary makes evident that the behavior of $[4Fe\text{-}4S/Se]^+$ synthetic and native clusters is far more intricate and perplexing than could have been imagined just a few years earlier. Such behavior is not the object of mere curiosity inasmuch as the Fd_{ox}/Fd_{red} electron-transfer couple ($[4Fe\text{-}4S]^{2+,+}$) is one of the most pervasive in biology. As such, it is imperative to understand the properties of both oxidation states as thoroughly as possible. Our most recent work[10-12] resulted in the recognition of behavioral categories i–iii above. Of these, the spin-admixed category was documented primarily with one example, $(Et_4N)_3[Fe_4S_4(SCH_2Ph)_4]$. Here we provide evidence for additional members of this category with emphasis on the new cluster compound $(Et_4N)_3[Fe_4S_4(S\text{-}o\text{-}C_6H_4StBu)_4]$, whose structure and electronic properties are reported. Also described are the magnetic and Mössbauer spectroscopic properties of several other reduced clusters that also currently appear to be best placed in the spin-admixed category.

Experimental Section

Preparation of Compounds. The compounds $(Et_4N)_3[Fe_4S_4(StBu)_4]\cdot MeCN$ and $(Me_4N)_3[Fe_4S_4(SEt)_4]$ were prepared by the single-step synthesis of reduced clusters,[2] and $(Et_3NMe)_3[Fe_4S_4(SPh)_4]$ was obtained by reduction of the dianionic cluster with sodium acenaphthylenide in acetonitrile.[1]

2-(*tert*-Butylthio)benzenethiol. The precursor, *tert*-butyl phenyl sulfide, was prepared as described by Babin et al.[27] using the generalized method of Cain et al.[28] To 145 mL (0.96 mol) of *N,N,N'N'*-tetramethylethylenediamine in a flame-dried flask was added 80.0 g (0.48 mol) of *tert*-butyl phenyl sulfide. The solution was degassed, cooled to 0 °C, and treated with 1.1 equiv (0.53 mol) of *n*-butyllithium via cannula. This solution was stirred for 1 h at room temperature and for ${}^1/_2$ h at 45 °C, resulting in a cream-colored suspension. This was cooled to 0 °C, and 17.0 g (0.53 mol) of elemental sulfur was added slowly, forming a yellow-orange solution after the reaction mixture was warmed to room temperature. The mixture was quenched with 1 M HCl and multiply extracted with hexanes. The organic extracts were washed with aqueous KOH, and the aqueous component was acidified and extracted with hexanes. The combined organic extracts were washed (brine) and dried (Na_2SO_4), and the solvent was removed. Distillation of the remainder at 89–90 °C/0.15 Torr afforded 69.9 g (73%) of pure thiol. ^1H NMR ($CDCl_3$): δ 1.35 (9, s, *t*Bu), 4.90 (1, s, SH), 7.06 + 7.19 (2, *t*, 4- and 5-H), 7.37 + 7.53 (2, d, 3- and 6-H).

The following preparations were carried out under strictly anaerobic conditions; solvents were degassed before use.

$(Et_4N)_2[Fe_4S_4(S\text{-}o\text{-}C_6H_4StBu)_4]$. To a solution of 3.00 g (3.09 mmol) of $(Et_4N)_2[Fe_4S_4(StBu)_4]$[29] in 50 mL of acetonitrile was added a solution of 2.46 g (12.4 mmol) of 2-(*tert*-butylthio)benzenethiol in 25 mL of acetonitrile. This solution was stirred for 1 h, after which solvent was removed in vacuo. The residue was dissolved in 50 mL of acetonitrile, the solution was filtered, and the filtrate was layered with 100 mL of ether. The oily residue that deposited was separated from the filtrate. It was washed with methanol and ether and dried in vacuo to afford 3.0 g (69%) of product as a thick red-brown oil. This material was not analyzed and was used directly in the synthesis of the reduced cluster. The product was shown to be substantially pure, and the cluster was identified, by its NMR spectrum.[8] ^1H NMR (CD_3CN, 298 K): δ 1.57 (9, *t*Bu), 5.08 (1, *p*-H), 6.00 (1, *o*-H), 8.46 + 8.55 (2, *m*-H).

$(Et_4N)_3[Fe_4S_4(S\text{-}o\text{-}C_6H_4StBu)_4]$. To a solution of 3.00 g (2.14 mmol) of the preceding cluster in 100 mL of THF was added 0.35 g (2.14 mmol) of Et_4NCl. A solution of 1.2 equiv of sodium acenaphthylenide in THF (from sodium and acenaphthylene) was introduced with stirring, resulting in the separation of a brown solid. This material was collected and dissolved in 100 mL of acetonitrile, and the solution was filtered. Cooling the filtrate to −20 °C caused separation of solid, which was collected by filtration and dried in vacuo, affording 1.47 g (45%) of pure product as black microcrystals. Anal. Calcd for $C_{64}H_{112}Fe_4N_3S_{12}$: C, 50.18; H, 7.37; N, 2.74. Found: C, 50.27; H, 7.53; N, 2.73. ^1H NMR ($Me_2SO\text{-}d_6$, 298 K): δ −0.22 (1, *o*-H), 1.61 (9, *t*Bu), 11.0 + 11.4 (2, *m*-H).

Reduced clusters are extremely sensitive to oxidation, especially in solution. Their isotropically shifted ^1H NMR spectra[8] are very responsive to even slight extents of oxidation and were used to establish that all compounds subject to the measurements below were fully reduced. The solvate composition of $(Et_4N)_3[Fe_4S_4(StBu)_4]\cdot MeCN$ was checked by NMR signal integration in $Me_2SO\text{-}d_6$, a necessary procedure inasmuch as solvated and desolvated cluster compounds can possess different ground states.[12]

Physical Measurements. All measurements were performed under strictly anaerobic conditions. Magnetic susceptibility and magnetization measurements at applied fields of 5 kOe and up to 50 kOe, respectively, were carried out on an SHE 905 SQUID magnetometer operating between 1.8 and 300 K. Finely ground samples of ca. 20–30 mg were loaded into precalibrated containers and sealed under a N_2/He atmosphere with epoxy resin. For $(Et_4N)_3[Fe_4S_4(S\text{-}o\text{-}C_6H_4StBu)_4]$, samples were dispersed in frozen toluene to inhibit crystallites from orienting in large applied fields at low temperatures. Duplicate samples were reproducible to ±2% at all values of the applied field. Diamagnetic susceptibility corrections for the sample and toluene were applied with the use of tabulated constants.[30] Mössbauer spectra were determined with a constant-acceleration spectrometer equipped with a ^{57}Co source in a Rh matrix. Magnetically perturbed spectra were obtained in longitudinally applied fields up to 80 kOe with the source and absorber at 4.2 K. Zero-field measurements were made at 4.2 and 80 K with the spectrometer operating in the time mode and the source maintained at room temperature. Polycrystalline samples were dispersed in boron nitride powder and sealed in plastic sample holders.

Collection and Reduction of X-ray Data. Large black blocks of $(Et_4N)_3[Fe_4S_4(S\text{-}o\text{-}C_6H_4StBu)_4]$ were obtained by slow cooling of an acetonitrile solution. A crystal was sealed in a glass capillary under a dinitrogen atmosphere. Data collection was carried out on a Nicolet P3F automated four-circle diffractometer equipped with a graphite monochromator. Crystal data are provided in Table I. The orientation and unit cell dimensions were obtained from 25 machine-centered reflections ($20° \le 2\theta \le 25°$). Intensities of three check reflections monitored every 123 reflections revealed no significant decay over the course of data collection. The data set was processed with the program XTAPE of the SHELXTL program package (Nicolet XRD Corp., Madison, WI), and an empirical absorption correction was applied with the program PSICOR. Axial photographs and the systematic absences $h0l$ ($h + l = 2n + 1$) and $0k0$ ($k = 2n + 1$) uniquely identify the space group as $P2_1/n$ (No. 14).

Structure Solution and Refinement. Atomic scattering factors were taken from tabulated data.[31] The Fe and bridging S atoms were located by the direct-methods program MULTAN.[32] All remaining non-hydrogen atoms were found by Fourier maps and refined by using CRYSTALS.[33] The asymmetric unit consists of one anion and three cations. No disorder was evident in core atom positions; however, the carbon atoms of *tert*-butyl groups required large thermal ellipsoids, indicating some disorder

Table I. Crystallographic Data for $(Et_4N)_3[Fe_4S_4(S\text{-}o\text{-}C_6H_4StBu)_4]$

chem formula: $C_{64}H_{112}Fe_4N_3S_{12}$	space group: $P2_1/n$ (No. 14)
fw = 1531.13	T = 297 K
a = 17.467 (7) Å	λ = 0.71069 Å (Mo Kα)
b = 15.011 (7) Å	ρ_{calcd} = 1.28 g/cm^3
c = 30.413 (9) Å	μ = 10.3 cm^{-1}
β = 94.31 (3)°	$R(F_o)$ = 0.0793
V = 7952 (5) Å^3	$R_w(F_o)$ = 0.0807
Z = 4	

(20) Moulis, J.-M.; Meyer, J.; Lutz, M. *Biochem. J.* **1984**, *219*, 829.
(21) Moulis, J.-M.; Meyer, J. *Biochemistry* **1984**, *23*, 6605.
(22) Gaillard, J.; Moulis, J.-M.; Meyer, J. *Inorg. Chem.* **1987**, *26*, 320.
(23) Auric, P.; Gaillard, J.; Meyer, J.; Moulis, J.-M. *Biochem. J.* **1987**, *242*, 525.
(24) (a) Lindahl, P. A.; Day, E. P.; Kent, T. A.; Orme-Johnson, W. H.; Münck, E. *J. Biol. Chem.* **1985**, *260*, 11160. (b) Meyer, J.; Gaillard, J.; Moulis, J.-M. *Biochemistry* **1988**, *27*, 6150.
(25) Lindahl, P. A.; Gorelick, N. J.; Münck, E.; Orme-Johnson, W. H. *J. Biol. Chem.* **1987**, *262*, 14945.
(26) Hales, B. J.; Langosch, J.; Case, E. E. *J. Biol. Chem.* **1986**, *261*, 15301.
(27) Babin, D.; Fourneron, J. D.; Harwood, L. M.; Julia, M. *Tetrahedron* **1981**, *37*, 325.
(28) Cain, M. E.; Evans, M. B.; Lee, D. F. *J. Chem. Soc.* **1962**, 1694.
(29) Mascharak, P. K.; Hagen, K. S.; Spence, J. T.; Holm, R. H. *Inorg. Chim. Acta* **1983**, *80*, 157.
(30) O'Connor, C. J. *Prog. Inorg. Chem.* **1982**, *29*, 203.
(31) Cromer, D. T.; Waber, J. T. *International Tables for X-ray Crystallography*; Kynoch: Birmingham, England, 1974.
(32) Main, P.; Fiske, S. J.; Hull, S. E.; Lessinger, L.; Germain, G.; Declerq, J.-P.; Woolfson, M. M. "MULTAN-80, A System of Computer Programs for the Automatic Solution of Crystal Structures from X-ray Diffraction Data", Universities of York and Louvain, 1980.
(33) Watkin, D. J.; Carruthers, J. R. "CRYSTALS Users' Manual", Chemical Crystallography Laboratory, Oxford University, 1984.

Table II. Positional Parameters (×10^4) for $(Et_4N)_3[Fe_4S_4(S\text{-}o\text{-}C_6H_4SC(CH_3)_3)_4]$ (**1**)

atom	x/a	y/b	z/c
Fe(1)	4227 (1)	1491 (2)	8523.4 (8)
Fe(2)	5004 (1)	1556 (2)	7772.9 (8)
Fe(3)	5778 (1)	1737 (2)	8572.4 (8)
Fe(4)	5153 (1)	126 (2)	8321.7 (8)
S(1)	4838 (3)	2675 (3)	8271 (2)
S(2)	4052 (3)	577 (3)	7910 (2)
S(3)	5140 (3)	806 (3)	9007 (1)
S(4)	6131 (3)	806 (3)	8004 (1)
S(5)	3039 (3)	1695 (4)	8771 (2)
C(50)	3105 (10)	2635 (9)	9109 (4)
C(51)	2464 (8)	3152 (11)	9178 (4)
C(52)	2527 (10)	3912 (11)	9437 (5)
C(53)	3235 (13)	4169 (10)	9635 (4)
C(54)	3871 (10)	3647 (13)	9573 (5)
C(55)	3810 (10)	2889 (12)	9310 (5)
S(9)	1540 (3)	2883 (5)	8959 (2)
C(56)	1101 (13)	2243 (16)	9373 (8)
C(57)	925 (17)	2859 (22)	9756 (11)
C(58)	1591 (19)	1512 (24)	9552 (10)
C(59)	387 (23)	1881 (24)	9176 (11)
S(6)	4961 (3)	2332 (3)	7125 (2)
C(60)	4741 (6)	1583 (9)	6683 (5)
C(61)	4441 (6)	1889 (10)	6272 (5)
C(62)	4238 (6)	1293 (12)	5934 (5)
C(63)	4340 (6)	387 (11)	6009 (6)
C(64)	4642 (6)	81 (10)	6415 (6)
C(65)	4844 (6)	678 (10)	6748 (5)
S(10)	4203 (3)	2988 (4)	6160 (2)
C(66)	5100 (11)	3603 (13)	6063 (6)
C(67)	4953 (13)	4055 (16)	5625 (8)
C(68)	5179 (15)	4327 (19)	6436 (9)
C(69)	5772 (15)	3052 (16)	6081 (7)
S(7)	6641 (3)	2724 (4)	8895 (2)
C(70)	7396 (6)	2119 (10)	9168 (4)
C(71)	7850 (8)	2484 (10)	9519 (4)
C(72)	8409 (7)	1969 (12)	9745 (4)
C(73)	8529 (7)	1092 (12)	9624 (5)
C(74)	8082 (8)	724 (10)	9273 (5)
C(75)	7518 (7)	1238 (11)	9048 (4)
S(11)	7716 (3)	3574 (4)	9710 (2)
C(76)	8328 (10)	4273 (12)	9416 (6)
C(77)	8518 (18)	3886 (22)	8971 (11)
C(78)	9053 (19)	4438 (21)	9686 (10)
C(79)	7917 (25)	5143 (34)	9352 (12)
S(8)	5049 (3)	−1397 (3)	8315 (2)
C(80)	5798 (7)	−1847 (9)	8659 (3)
C(81)	5814 (8)	−2758 (9)	8740 (4)
C(82)	6405 (9)	−3122 (10)	9016 (4)
C(83)	6976 (8)	−2580 (12)	9213 (4)
C(84)	6958 (7)	−1673 (12)	9128 (4)
C(85)	6372 (7)	−1306 (9)	8854 (4)
S(12)	5073 (4)	−3365 (4)	8468 (2)
C(86)	5159 (12)	−4541 (14)	8609 (9)
C(87)	5851 (19)	−4967 (23)	8424 (9)
C(88)	4429 (21)	−4901 (25)	8370 (11)
C(89)	5162 (19)	−4705 (28)	9101 (14)

in their positions. In addition, axial photographs contained several low-intensity spots between lattice lines, suggesting some crystal twinning. Twinning may be the main reason for the slightly high R values. Owing to limitations in data, all *tert*-butyl methyl groups were refined isotropically. Isotropic refinement converged at $R = 0.102$. One carbon atom of one phenyl ring (C(80)) was also isotropically described inasmuch as anisotropic refinement produced a nonpositive thermal ellipsoid. All other non-hydrogen atoms were anisotropically refined. Phenyl rings and cations were restrained by the method of addition observational equations[34] until final refinement. Hydrogen atoms were included at 0.96 Å from, and with isotropic thermal parameters 1.2 times those of, bonded carbon atoms. A final difference Fourier map showed several peaks of ≈0.7 e/Å^3 in the vicinity of the disordered *tert*-butyl groups; other peaks were below 0.5 e/Å^3. Final R factors are given in Table I; positional parameters are listed in Table II.[35]

(34) Waser, J. *Acta Crystallogr.* **1963**, *16*, 1091.
(35) See paragraph at end of paper concerning supplementary material.

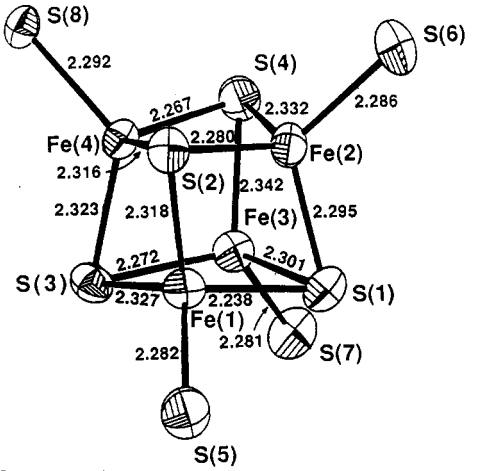

Figure 1. Structure of the Fe_4S_8 portion of cluster **1**, showing the atom-labeling scheme, 50% probability ellipsoids, and selected interatomic distances.

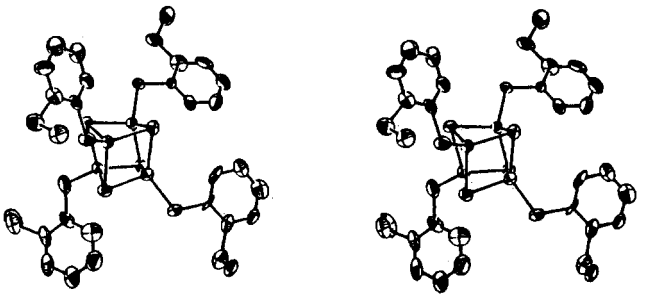

Figure 2. Stereoview of cluster **1**, showing 50% probability ellipsoids. Methyl groups of the 2-S*t*Bu substituents are omitted for clarity.

Results and Discussion

The reduced cluster compounds **1–9** are of primary interest in this work. Experimental results are reported for **1–4**; compound

$(Et_4N)_3[Fe_4S_4(S\text{-}o\text{-}C_6H_4S\text{t}Bu)_4]$ (**1**)
$(Et_4N)_3[Fe_4S_4(S\text{t}Bu)_4]\cdot MeCN$ (**2**)[2]
$(Et_3NMe)_3[Fe_4S_4(SPh)_4]$ (**3**)[1]
$(Me_4N)_3[Fe_4S_4(SEt)_4]$ (**4**)[2]
$(Et_4N)_3[Fe_4S_4(SCH_2Ph)_4]$ (**5**)[3]
$(Et_4N)_3[Fe_4S_4(S\text{-}p\text{-}C_6H_4Br)_4]$ (**6**)[4]
$(Me_4N)_3[Fe_4S_4(SPh)_4]\cdot 2MeCN$ (**7**)[11]
$(Me_4N)_3[Fe_4Se_4(SPh)_4]\cdot 2MeCN$ (**8**)[11]
$(Et_4N)_3[Fe_4S_4(SC_6H_{11})_4]\cdot 4MeCN$ (**9**)[12]

5 contains the only spin-admixed cluster documented previously.[12] The structure of cluster **1** is first examined; structures of **2–9** have already been reported. This cluster contains one of the larger and the most irregularly shaped terminal thiolate ligand(s) in any structurally defined Fe_4S_4 cluster. Because of the presence of the *o*-S*t*Bu group, the ligand departs from any semblance of symmetry about the C–S(Fe) bond and also has the potential for weak interaction with the Fe atoms. These factors raise the possibility of an intrinsically preferred ligand orientation arising from intracluster interactions rather than one set by crystal packing, in the event the two are not the same.

Structure of $[Fe_4S_4(S\text{-}o\text{-}C_6H_4S\text{t}Bu)_4]^{3-}$. The crystal structure consists of well-separated cations and anions with no unusually close contacts. The Fe_4S_8 portion of cluster **1** is depicted in Figure 1, and a stereoview of the entire cluster is provided in Figure 2. Selected interatomic distances and angles are contained in Table III. Angles are given in terms of ranges and mean values; individual values are not required in the structural description and are available elsewhere.[35]

No symmetry is imposed on cluster **1**, which has the familiar cubane-type $Fe_4(\mu_3\text{-}S)_4$ core, whose faces are nonplanar Fe_2S_2 rhombs. Core Fe–S distances divide rather clearly into sets of four "short" (2.238 (6)–2.280 (6), 2.265 (19) Å) and eight "long" (2.295 (6)–2.342 (6), 2.319 (23) Å) with the indicated ranges and

Table III. Selected Interatomic Distances (Å) and Angles (deg) for $[Fe_4S_4(S\text{-}o\text{-}C_6H_4StBu)_4]^{3-}$

Fe(1)–S(2)	2.318 (6)	Fe(1)–S(1)	2.238 (6)
Fe(1)–S(3)	2.327 (5)	Fe(2)–S(2)	2.280 (6)
Fe(2)–S(1)	2.295 (6)	Fe(3)–S(3)	2.272 (5)
Fe(2)–S(4)	2.332 (5)	Fe(4)–S(4)	2.267 (5)
Fe(3)–S(1)	2.301 (6)	mean	2.265 (19)
Fe(3)–S(4)	2.342 (6)		
Fe(4)–S(2)	2.316 (5)	Fe(1)–Fe(4)	2.710 (4)
Fe(4)–S(3)	2.323 (5)	Fe(2)–Fe(3)	2.706 (3)
mean	2.319 (23)	mean	2.708 (3)
		Fe(1)–Fe(2)	2.744 (3)
Fe(1)–S(5)	2.282 (6)	Fe(1)–Fe(3)	2.727 (4)
Fe(2)–S(6)	2.286 (5)	Fe(2)–Fe(4)	2.720 (4)
Fe(3)–S(7)	2.281 (6)	Fe(3)–Fe(4)	2.738 (4)
Fe(4)–S(8)	2.292 (5)	mean	2.732 (11)
mean	2.285 (5)		
S(5)–C(50)	1.744 (17)		
S(6)–C(60)	1.772 (14)		
S(7)–C(70)	1.759 (14)		
S(8)–C(80)	1.750 (13)		
mean	1.756 (12)		

	range	mean
Fe–Fe–Fe	59.29 (9)–60.71 (9)	60.00 (5)
S–Fe–S	102.8 (2)–107.5 (2)	104.9 (1.6)
Fe–S–Fe	70.8 (2)–74.5 (2)	72.6 (1.0)
S–Fe–SR[a]	101.5 (5)–120.6 (2)	

[a] Angles external to Fe_4S_4 core.

mean values. This arrangement corresponds to a *compressed* tetragonal core distortion from idealized T_d symmetry. As such, an idealized $\bar{4}$ axis passes through the centers of faces Fe(2,3)-S(1,4) and Fe(1,4)S(2,3). The short and long bonds are roughly parallel and perpendicular, respectively, to this axis. Nonbonded S···S distances also reflect the distortion as they divide into sets of two long (mean 3.731 (7) Å) and four short (mean 3.609 (26) Å) that are located perpendicular and parallel, respectively, to the $\bar{4}$ axis.

Dimensions of the Fe_4 core fragment are also biased toward a tetragonal distortion, there being two short (2.708 (3) Å) and four long (2.732 (11) Å) Fe–Fe distances with the short distances perpendicular to the $\bar{4}$ axis. Compared to those of other reduced clusters except **7**, Fe–Fe distances are short, with no bond longer than 2.744 (3) Å and a mean value of 2.724 (15) Å. This produces a relatively small Fe_4 tetrahedron (2.38 $Å^3$), which contributes to the smallest core volume (9.57 $Å^3$) yet observed for reduced clusters. In the set **1**–**9**, the largest core volume (9.98 $Å^3$, **9**) exceeds the smallest by 4.3%. The corresponding value for $[4Fe\text{-}4S]^{2+}$ cores is only 2.0%. This fact serves to accentuate the softness and pliability of the reduced core.

The terminal Fe–S bonds in **1** average to 2.285 (5) Å, a value larger than corresponding mean values in oxidized clusters and consistent with the larger Fe(II) character of the reduced core. As in other cluster structures, the S–Fe–S* angles, external to the core (S* is a core atom), are variable and reduce the local symmetry at Fe sites below C_{3v}. At each Fe atom there is one small angle (100–106°) and two substantially larger ones (116–120°). The small angles are S(5)–Fe(1)–S(2), S(6)–Fe(2)–S(1), S(7)–Fe(3)–S(1), and S(8)–Fe(4)–S(2); all involve one long Fe–S core bond and are related by the $\bar{4}$ axis. A useful structural parameter is the dihedral angle β = S*–Fe–S–C, of which there are three at each Fe site. When one of these angles is 180°, illustrated as follows, the thiolate group is placed in a staggered configuration, i.e., as far from the core Fe–S* edges as possible.

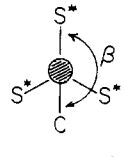

Inspection of Figure 2 shows that this situation is closely approached at each site; β = 160, 162, 174, and 178°. This arrangement doubtless arises from the steric demands of the *o*-S*t*Bu group, which is not coordinated but is disposed at a maximum distance from the core. We conclude that the observed ligand conformations are largely or completely set by intracluster interactions.

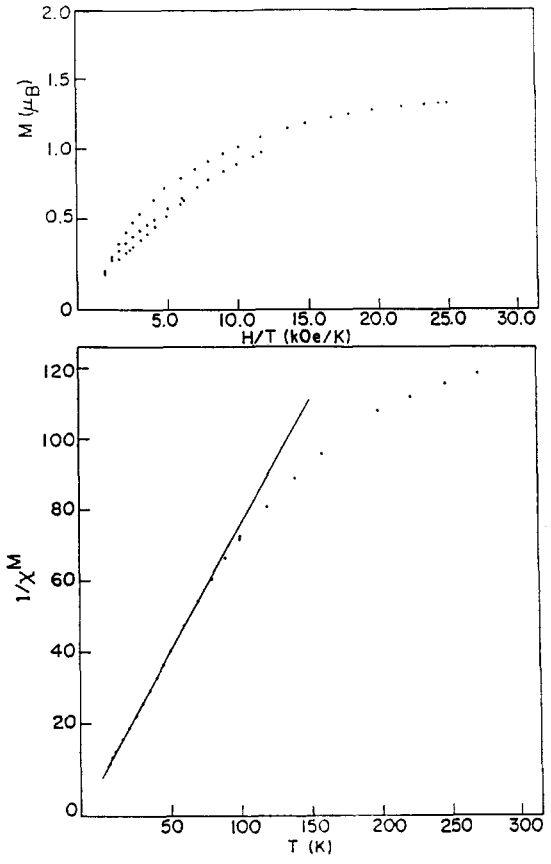

Figure 3. Magnetization (top) and magnetic susceptibility (bottom) of cluster **1**. In this and succeeding figures, magnetization curves in ascending order refer to applied fields of 12.5, 25, and 50 kOe, and the straight line is a fit to the Curie–Weiss region using the parameters in Table IV.

Electronic Properties. The magnetic and spectroscopic properties of the prototypical spin-admixed cluster **5** have been described in detail in recent work.[12] This cluster is distinguished from those in categories i and ii by the absence of EPR and Mössbauer spectroscopic features from $S = {}^1/_2$ and/or $S = {}^3/_2$ state(s). A particularly distinctive feature is the absence of $S = {}^1/_2$ Mössbauer signatures at ca. +3 and −2 mm/s in large applied fields. Properties of clusters **1**–**4** are considered next in regard to their ground-spin-state classification.

(a) Magnetic Behavior. The magnetic susceptibility and magnetization properties of clusters **1**–**3** are depicted in Figures 3–5. Magnetic parameters resulting from fits of the low-temperature susceptibilities to the Curie–Weiss law are given in Table IV. For pure $S = {}^1/_2$ and $S = {}^3/_2$ states the Curie constant C = 0.375 and 1.875 emu K/mol, respectively, when g_e = 2. Compared to that of other reduced clusters,[12] the behavior of **1** is unusual due to its large Weiss constant (−6.45 K). The Curie constants and the initial slopes of the magnetization plots are intermediate between those expected for spin-doublet and -quartet states. These results eliminate pure spin states but are consistent with the following $S = {}^1/_2{:}{}^3/_2$ spin state ratios: 31%:69% (**1**), 46%:54% (**2**), 80%:20% (**3**). The magnetization data for **2** (Figure 4) can be satisfactorily fit, by using the procedure described elsewhere,[12] with this ratio and the parameters D = −6.0 cm^{-1} and $|E/D|$ = 0.16. The magnetization data for **1** and **3** were not similarly analyzed. However, by comparison to the data for physical mixtures of pure spin states[12] (e.g., $(Et_4N)_3[Fe_4S_4(SR)_4]$, R = Me, Et), the magnetic properties of the two clusters (intermediate Curie constants and initial magnetization slopes, and

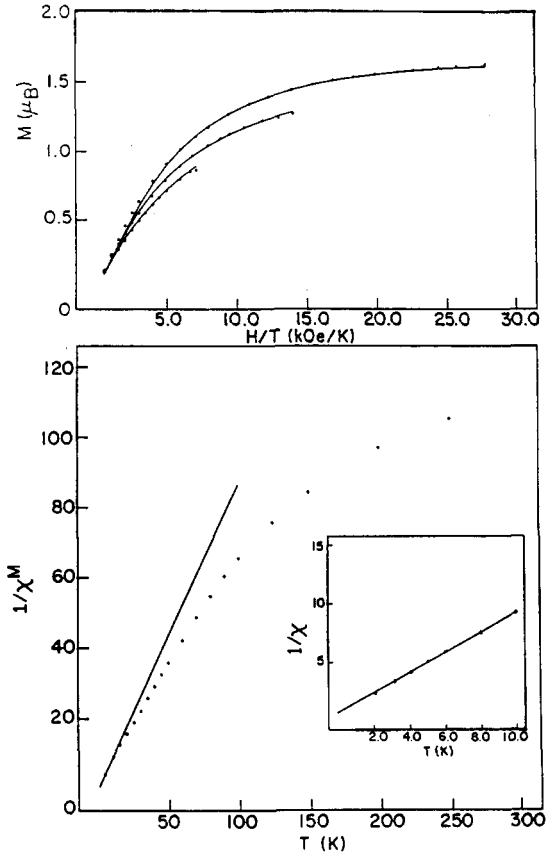

Figure 4. Magnetization (top) and magnetic susceptibility (bottom) of cluster **2**. The inset is the susceptibility plot showing the Curie behavior at 2.0–10 K measured in an applied field of 100 Oe.

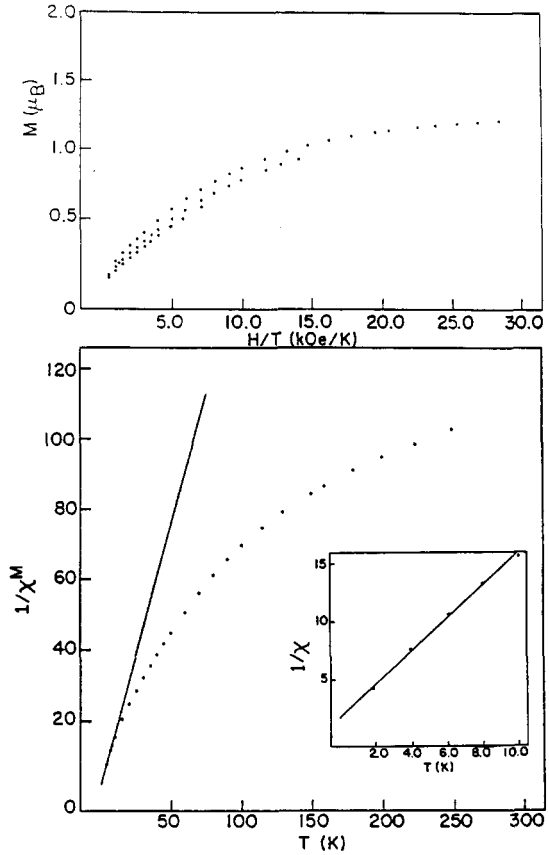

Figure 5. Magnetization (top) and magnetic susceptibility (bottom) of cluster **3**.

saturation magnetization) are not inconsistent with a physical mixture description.

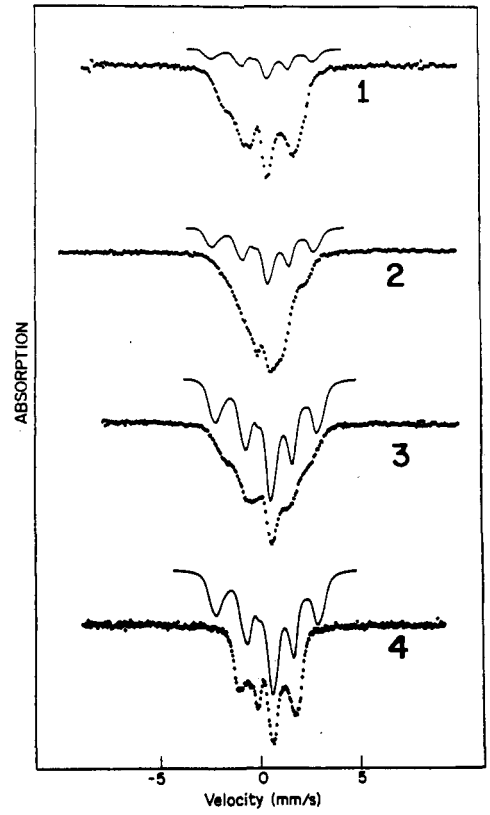

Figure 6. Mössbauer spectra of polycrystalline clusters **1–4** determined in an applied field of 60 kOe at 4.2 K. Above the spectra of **1–3** are given $S = {}^1/_2$ spectra at 60 kOe scaled to the percentage of doublet spin state determined from magnetic susceptibility data (see text). Above the spectrum of **4** is an unweighted $S = {}^1/_2$ spectrum; the spin-doublet spectra are the same except for weighting factors.

The magnetic properties of **4** (not shown) are the most unusual of all reduced clusters thus far studied. At low temperatures and small applied fields (<10 K, 100 Oe), the magnetic susceptibility does not display Curie or Curie–Weiss behavior and μ_{eff} steadily increases from 1.7 μ_B at 3.0 K to 2.58 μ_B at 10 K. The magnetization is characterized by an apparent saturation value of ≈0.8 μ_B at 50 kOe and 1.8 K. No simple model based on any pure spin state or a physical mixture of pure spin states can reproduce this behavior.[36] We offer no classification of the ground state of this cluster.

(b) Mössbauer Spectroscopy. Parameters from fits of the zero-field spectra (not shown) are contained in Table IV. Values of the isomer shifts and quadrupole splittings are entirely comparable to those of other synthetic and most biological clusters at the [4Fe-4S]$^+$ oxidation level. As will be seen, Mössbauer spectroscopy is particularly useful in identifying the spin-admixed ground-state category.

Magnetic Mössbauer spectra of clusters **1–4** are presented in Figure 6. Above the spectra of **1–3** are included spectra at 60 kOe for the $S = {}^1/_2$ state, which have been scaled to the proportion of that state, that produced adequate fits to the low-temperature

(36) We note, however, that intercluster exchange interactions might be partially responsible for the somewhat anomalous magnetic behavior. This is the only cluster, of the many that we have examined, that does *not* follow the Curie or Curie–Weiss law at low temperatures. All other cluster compounds have nonzero Θ values, and for all but **1**, Θ ≤ 1.6 K, and in some cases, <1 K.[11,12] There is no relationship between the sign or value of the Weiss constant and spin-admixed behavior, inasmuch as clusters belonging to categories i and ii have values comparable to those of **2** and **3**.[12] We are cognizant of the fact that the spin-admixed condition has been detected only in the solid state, where weak intercluster exchange effects are possible. If nonzero Θ values are ascribed to such effects, it is not apparent that these effects alone cause spin-admixed behavior. Note that the prototype spin-admixed cluster compound, **5**, has a very small Weiss constant (Θ = −0.44 K) and follows the Curie–Weiss law at 2–10 K and an applied field of 100 G.[12] We do not know the origin of the relatively large Θ value of **1**.

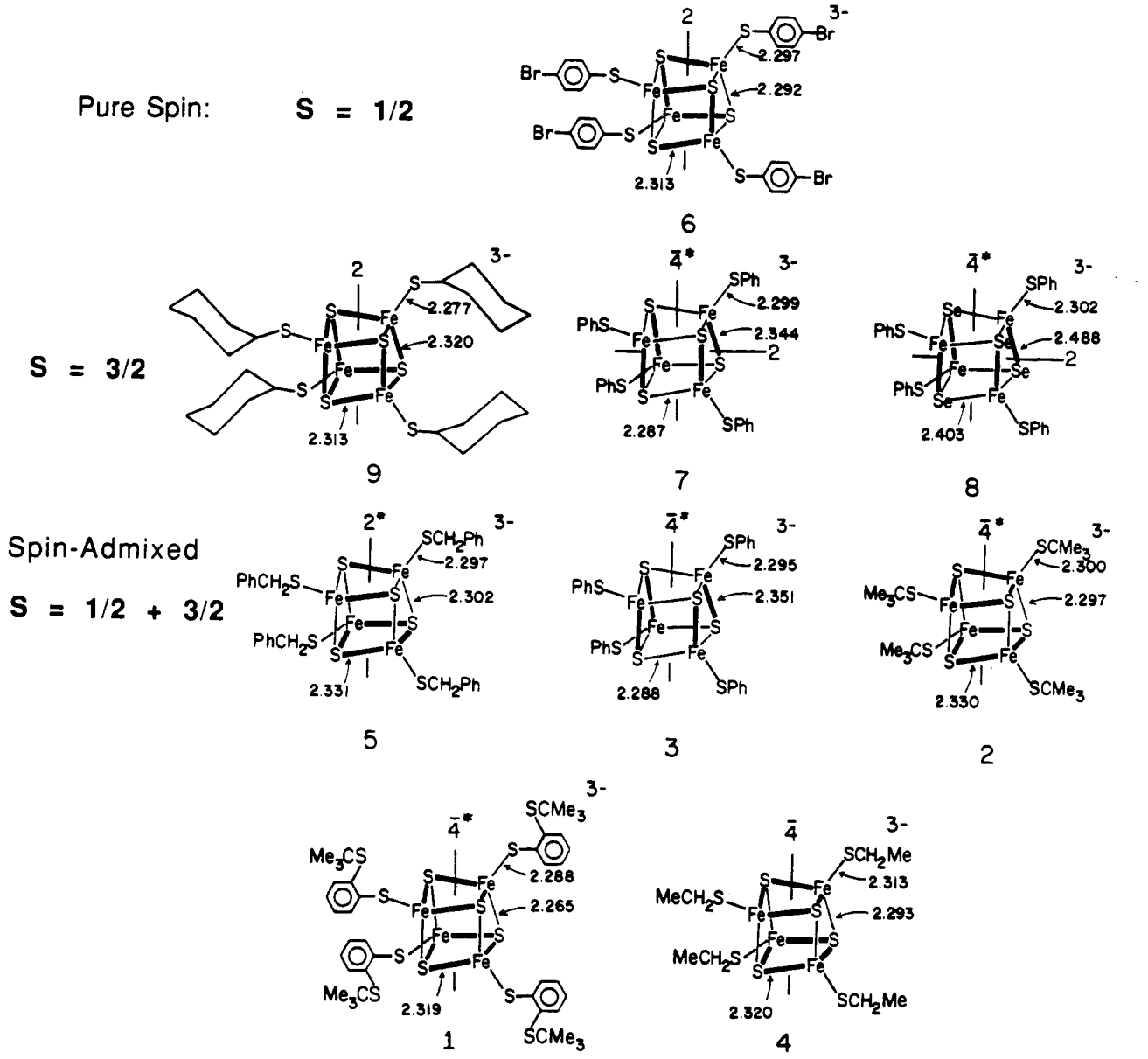

Figure 7. Schematic depiction of the cluster structures of compounds arranged according to the spin-state classifications made in this and previous work.[12] Mean values (Å) of short and long (bold line) Fe–S core bonds and Fe–S terminal bonds are given. Crystallographically imposed and idealized (*) symmetry axes are indicated.

Table IV. Electronic Properties of Spin-Admixed Clusters

property	1	2	3	4
$\chi^M = C/(T-\Theta)$				
T range, K	6.0–70	2.0–10	2.0–15	*a*
C, emu K/mol	1.411	1.189	0.702	
Θ, K	6.45	−0.93	−1.20	
δ,[b] mm/s	0.48	0.45	0.44	0.44
	0.48	0.48	0.48	
ΔE_Q,[b] mm/s	1.35	0.93	1.01	1.12
	1.15	1.74	1.78	

[a] No discernible Curie region. [b] Determined at 4.2 K. Isomer shifts are referenced to Fe metal at 4.2 K; to refer to Fe metal at room temperature, add 0.12 mm/s. When two sites are given, the relative intensities are 1:1; parameters for a given doublet are in order.

magnetic susceptibility data. For **4**, which does not show a well-defined Curie region, an unscaled $S = {}^1/_2$ spectrum is included. Note the definite absence of the $S = {}^1/_2$ signatures in the outer wings of the spectrum of **4**. Indeed, none of the spectra in Figure 6 possess clearly resolved outer wings that are indicative of the $S = {}^1/_2$ state in synthetic or native pure-spin clusters or in physical mixtures. All $S = {}^3/_2$ synthetic[1,5,10-12] and native[24-26] clusters are characterized by collapsed Mössbauer spectra in large applied fields with an overall spread of about 3 mm/s. These spectra do not interfere in outer-wing regions where the $S = {}^1/_2$ absorptions occur.

For clusters **2** and **3**, the poorly resolved shoulders on the sides of the central absorption could conceivably arise from $S = {}^1/_2$ species. However, if this were the case, these species would have to possess hyperfine fields that are ca. 40% smaller than those exhibited by all known synthetic and biological spin-doublet clusters. All pure synthetic[12] and native[24,37,38] $S = {}^1/_2$ clusters have been shown to possess virtually identical magnetic Mössbauer spectra (at 60 kOe) with very little variation in the positions of the outer wings. Also, the outer $S = {}^1/_2$ Mössbauer features in the spectra of physical mixtures[12] are in positions indistinguishable from those of pure-spin clusters. For **2**, not only would the hyperfine fields have to be reduced, but the overall percentage of this anomalous $S = {}^1/_2$ contribution would have to be increased by 10% over that found from magnetic properties, in order to account satisfactorily for the shoulder on the high-velocity side

(37) Middleton, P.; Dickson, D. P. E.; Johnson, C. E.; Rush, J. D. *Eur. J. Biochem.* **1978**, *88*, 135.
(38) Christner, J. A.; Münck, E.; Janick, P. A.; Siegel, L. M. *J. Biol. Chem.* **1981**, *256*, 2098.

of the central absorption. In the case of **1**, the $S = {}^1/_2$ state percentage in a physical mixture would be smaller than those for **2–4**. Careful inspection of the spectrum of this cluster reveals no discernible features, particularly on the high-velocity side, that correspond to the $S = {}^1/_2$ state.

On the basis of the foregoing evidence, clusters **1–4** are placed in spin-admixed category iii. *These clusters do not possess Mössbauer spectra that are simple summations of pure* $S = {}^1/_2$ *and* $S = {}^3/_2$ *spectra.* At present, there is no theoretical description of spin-admixed cluster ground states; we have given a qualitative description of such a state.[12] Maltempo[39] has proposed a spin-admixed ground state for bacterial ferricytochrome *c'*.

While it may be possible for clusters **1–3** to contain $S = {}^1/_2$ components, such species would have to possess hyperfine fields that are significantly smaller than those exhibited by all known spin-doublet synthetic and biological clusters. The near-constancy of $S = {}^1/_2$ Mössbauer magnetic spectra is the basis for our classification of **1–4**. Also, we cannot exclude small fractions of clusters with $S > {}^3/_2$, but no such synthetic cluster has yet been identified. A very small percentage of a $S = {}^5/_2$ cluster in ATP-bound Av2 has been detected by EPR spectroscopy;[25] no Mössbauer spectrum of a spin-sextet cluster is known. The $S = {}^7/_2$ cluster in Se-Fd$_{red}$ shows Mössbauer features at ca. −4 and +5 mm/s at 50 kOe.[23] This is the only example of a cluster with the $S = {}^7/_2$ state; consequently, the variability of the spectrum is unknown. Features at or near −4 and +5 mm/s are clearly absent in the spectra of the present clusters.

Structures and Spin States. Presented in Figure 7 are schematic depictions of the nine known structures of $[Fe_4S_4(SR)_4]^{3-}$ clusters, all determined at room temperature. On the basis of the partitioning of Fe–S core bonds into long and short categories, *five* distinct core distortions from T_d symmetry are recognized. The existence of these distortions certainly means that crystalline forces influence stereochemistry. As indicated by the variability of S–Fe–S* angles, these forces most likely manifest themselves by interactions with terminal thiolate ligands. The most frequent distortions thus far encountered are compressed (**1**, **2**, **4**) and elongated (**3**, **7**, **8**) tetragonal, found in three cases each. We have argued that ligand conformations in **1** are intrinsic, implying that the core distortion is also intrinsic to that cluster. We consider it less certain that this is true of ligand conformations and core structures in other cases, but note that the conformational angles in **2** (β = 166–175°) are close to those in **1**.[40] However, the presence of four nearly staggered ligand conformations does not necessarily relate to core shape inasmuch as elongated **8** (169, 179°) and **5** (162–180°), with opposite and different types of distortion, respectively, have comparable arrangements. Further, elongated **3**, in two different crystalline environments[1] (151–180, 136–175°), has one ligand that markedly departs from the staggered conformation. The picture that emerges for the [4Fe-4S]$^+$ core in its various clusters is that of a potential energy surface with a series of minima of nearly equal stabilities, i.e., core structural *plasticity*. While the compressed tetragonal core structure may be the inherently stable one for cluster **1**, the innately stable structure of the reduced core is not yet proven. Of course, this may be a moot point if, as current evidence suggests, structural energy minima are very closely spaced.

As also may be seen from Figure 7, there is no unifying relation between core structure and spin state. The collective results show that there does not exist a unique core distortion or a unique set of thiolate ligand orientations (or a combination of the two) that is indicative of spin-admixed behavior in clusters **1–5**. An equivalent statement applies to pure $S = {}^3/_2$ clusters **7–9**. However, these clusters do possess terminal ligand conformational angles in the 160–180° range. These observations are offered with the qualification that crystal structures are known at ambient temperature and magnetic and Mössbauer spectroscopic properties are determined at cryogenic temperatures. The present results, when taken with those reported earlier, substantiate three types of ground-state behavior of reduced clusters by providing additional examples in the spin-admixed category. Thus far, no native cluster with a spin-admixed ground state has been detected. As the understanding of the electronic structures of reduced clusters is advanced, the term "spin-admixed" may prove to be imprecise. Here and previously,[12] we apply it as a descriptor of that set of clusters that lack the defining properties of categories i and ii. As we have recently observed,[12] acquisition of structures at very low temperatures is the next necessary step in investigating any structure/property relations of synthetic analogues of reduced native clusters.

Acknowledgment. This research was supported at Harvard University by NIH Grant GM 28856 and at MIT by the National Science Foundation. We thank Dr. T. D. P. Stack for experimental assistance and useful discussions.

Registry No. **1**, 119679-58-2; **2**, 91294-56-3; **3**, 63115-84-4; **4**, 91294-59-6; HS-*o*-C_6H_4S*t*Bu, 119640-12-9; $(Et_4N)_2[Fe_4S_4(S\text{-}o\text{-}C_6H_4S$*t*$Bu)_4]$, 119656-27-8; $(Et_4N)_2[Fe_4S_4(S$*t*$Bu)_4]$, 62873-87-4; *tert*-butyl phenyl sulfide, 3019-19-0; sulfur, 7704-34-9.

Supplementary Material Available: Tables of intensity collection and structure refinement parameters, positional parameters, interatomic distances and angles, temperature factors, and calculated hydrogen atom positions for compound **1** and magnetic susceptibilities for compounds **1–4** (19 pages); a listing of structure factors for compound **1** (35 pages). Ordering information is given on any current masthead page.

(39) Maltempo, M. M. *J. Chem. Phys.* **1974**, *61*, 2540.

(40) Compressed cluster **4** is unusual in that it has the thiolate carbon atoms disordered over two positions throughout the crystal lattice, producing one staggered (171°) orientation and one with a smaller (145°) dihedral angle.[2] With this compound, it is unknown whether certain clusters have all thiolates staggered, while others have all thiolates possessing the smaller dihedral angle, or whether both orientations exist in the same cluster; thus, this case is not readily interpretable.